蠕動微型幫浦用 UV 固化膠粘劑的製作

*許藝菊、李杰瑞、李曉薇
南臺科技大學機械工程系
yichu@stust.edu.tw

摘 要

本文使用 UV 固化膠粘劑（NOA81）作為粘接材料和微結構材料，來製造蠕動式微型泵。NOA81 的最高強度是要接受 10.18 焦耳/平方米的能量後達到，以 UV 燈之強度換算是在 7 分鐘時間的紫外線固化，而在參數最佳化發現，後續加上 50℃、12 小時的加熱板加熱．會比單純光照更穩定；其次以 NOA81 做為微結構需的研究，本實驗測試的固化時間包括 1 分鐘，5 分鐘，至 60 分鐘。根據該測量，為 10 分鐘的樣品最佳，其幾何誤差為低於最大耐受（10%），而其他較短和較長的固化時間分別為 10%以上。在顯微鏡下觀測到在流道位置，最大的實驗量測標準差為 4.611 微米，對於腔室位置深度的標準偏差為 0.514 微米，這是非常小的。它顯示了 NOA81 在製造微流體的流道和腔室在幾何形狀的一致性與轉印時幾何形狀的忠實度。此外，本研究使用刀片試驗來驗證 NOA81 的接合強度，利用以表面能公式將裂紋長度計算出粘接強度。最後，應用於製造蠕動式微型泵，並測試其效能。實驗結果微型泵的最高薄膜位移和流量分別是 0.824 微米和 21.87 微升/分鐘，而最大背壓為 4.42 帕．與前期研究相同設計的 PMMA 熱壓型微型泵相較，此型的流量較小，因為該微型泵的通道較淺。另外，NOA81 材料具有比 PMMA 材料低的楊氏係數，在致動過程中，NOA81 結構變形也造成較小的背壓。

關鍵詞：接合強度, 紫外線固化膠粘劑, 蠕動微泵

Fabrication of a Peristaltic Micropump with UV Curable Adhesive

***Yi-Chu Hsu, Jeffrey Levin, Hsiao-Wei Lee**
Department of Mechanical Engineering, Southern Taiwan University of Science and Technology

Abstract

This study fabricates a peristaltic micropump using UV curable adhesive (NOA81) as bonding material and microchannel structure. First of all, the highest bonding strength of NOA81 is 10.18 J/m^2, achieved at 7 minutes by UV. The micropump's main body was fully cured for 7 minutes and heated on a hotplate for 12 hours at 50^{o}C for stabilization. Secondly, the curing times for these experiments include 1 minute, 5 minutes, up to 60 minutes. According to the measurements, geometrical errors for 10 minute samples were below the maximum tolerance (10%), while the other samples were above 10%. Standard deviation for each target area was compared. For channel area, the biggest standard deviation is 4.611 μm, while standard deviation for chamber area is 0.514 μm, and these values are very small compared to depth values. This shows the consistency of the NOA81 to replicate microstructure. Razor blade test was utilized to measure NOA81 bonding strength. Finally, the pump performance fabricated by NOA81 with optimal curing process was tested. The highest membrane displacement and flow rate of the NOA81 based micropump are 0.824 μm and 21.87 μl/min, respectively, while the maximum backpressure is 4.42 Pa. The flow rate is small because the micropump's channels are shallow and the shallow channels will produce high fluidic resistance. NOA81 structure also has low Young's Modulus. During actuation process, the NOA81 with low Young's Modulus structure undergoes a deformation, also making the backpressure smaller.

Keywords: UV Curable Adhesive, NOA81, Peristaltic Micropump

Received: Jan. 30, 2015; accepted: Sep., 2015.

Corresponding author: Y. -C. Hsu

I. Introduction

Micropumps are a fundamental component of microfluidic devices. Due to the wide range of applications such as drug delivery systems, electronic cooling systems, and fuel cells, many different types of micropumps have been developed. The majority of the micropump reported are diaphragm micropumps. The operational principles of a diaphragm micropump is based on the interactions between various mechanics. In a peristaltic micropump, sequential actuations of actuating diaphragms in a desired fashion can generate fluid flow rates in a controlled direction. The main advantage of a peristaltic micropump is that no valves or other internal parts ever touch running fluid. This advantage makes a peristaltic micropump become a good choice for drug delivery applications.

A number of peristaltic micropumps have been reported with various driving mechanisms such as piezoelectric, thermopneumatic, electromagnetic, pneumatic and electrostatic actuations [1,2]. Piezoelectric actuation is the most popular ones applied for peristaltic micropumps. The advantages are it has a short response time, a high output force at lower voltages and piezoelectric materials are commercially available. Thus, they can be easily integrated in micropump system.

The high demand for micropump is driving a need for a low cost fabrication for mass productions. New material such as UV curable adhesive is gaining recognition in microfluidic field. Compared to PDMS, these adhesives when fully cured have high solvent resistance and good adhesion to a substrate. Several researchers have published results in relation to the fabrication of microfluidic devices from UV curable products, such as NOA81 [3, 4, 5], NOA63 [6], NOA68 and NOA74 [7]. From these NOA adhesives types, NOA74 (80-95 cps) and NOA81 (300 cps) have lower viscosity than NOA63 and NOA68 [8]. The lower the viscosity, the easier it will be to deposit the UV adhesive on top of a substrate. NOA81 (90-Shore D) has higher hardness value rather than NOA74 (30-Shore D) [8]. In this work, PZT actuation was used as a driving mechanism and this actuation type has a high output force. The UV adhesive based structure should be able to withstand the high output force. Based on these reasons, NOA81 was chose to become the micropump's structure.

Bonding in microfluidic field is still quite challenging. The most common techniques include anodic bonding, chemical bonding, ultrasonic bonding and glue adhesive bonding. These techniques have some challenges in relation to cleanliness of the wafer, high temperature, oxidation and a chance for glue to flows in to the channels. One of the advantages from UV curable adhesive is that it can turn to its solid state with UV light curing in a short amount of time, thus preventing the glue to flows in to the channels.

In this paper, the fabrication process of the first workable peristaltic micropump ever made from UV curable adhesive is presented. There are three goals of the UV adhesive to serve in the peristaltic micropumps. They are durable, geometry accurate and able to transport actuation force to serve the function of a pump. The durability is first measured by razor blade test, which was performed to determine the bonding strength of the NOA81 and to detect any flaws in bonding process procedure. Next, NOA81 transfer characteristics were investigated by utilizing a confocal microscope. It was utilized to measure the geometrical changes of the micropump's structure between PMMA master mold and NOA81 structure mold. Finally, the UV adhesive based peristaltic micropump undergoes several experiments to determine its performance.

II. Experiments

1. Fabrication of The Peristaltic Micropump

PDMS was used as a mold during the transfer process because PDMS is more flexible than PMMA. Thus, during peeling, the UV adhesive based structure was able to peel off from PDMS mold without damaging the micropump's structure.

(1)PMMA Mold

The top view of the overall PMMA mold is shown in Fig. 2. The pattern of the mold is originally from silicon plate which was fabricated by standard MEMS, micro-electrical-mechanical system, process. The silicon chip is sacrificed to electroform a more durable nickel mold. The details are described in [13]. The microchannels width is expected to be 80 µm. The channels depths are varied on each spot (Fig. 4). The depths are 175.5 µm, 186.5 µm and 195.1 µm on CH 1, CH 2 and CH 3 spots, respectively. The depth differences between the three microchannels are owing to the non-uniform of the original PMMA master mold which is result from its multi-pattern-transform from a micro-machined silicon master mold and then a nickel pattern. The chambers depth is 15 µm. Hot embossing was utilized to fabricate the PMMA master mold. The detail of the process is described in [9].

(2) PDMS Mold

A mixture of silicon elastomer and a curing agent (Sylgard 184, Dow Corning) were mixed at 10:1 ratio. The mixture was stirred and placed in an oven to be degassed. Placed the PMMA mold on a flat surface and poured the degassed PDMS on top of PMMA master mold. Cure it in an oven at 90^{o}C for 1 hour.

(3)Transfer Process

NO81 was poured on top of PDMS mold using a pipette (0.25 cc). PMMA plate was brought into contact with PDMS mold, started at one end to draw the adhesive in and push air out. This method can prevent bubbles from appearing. The NOA81 with transferred microstructure was fully cured by UV light exposure (UVA 201-PO, 40 mW/cm) for 10 minutes. After that, peel off PMMA plate from the PDMS mold.

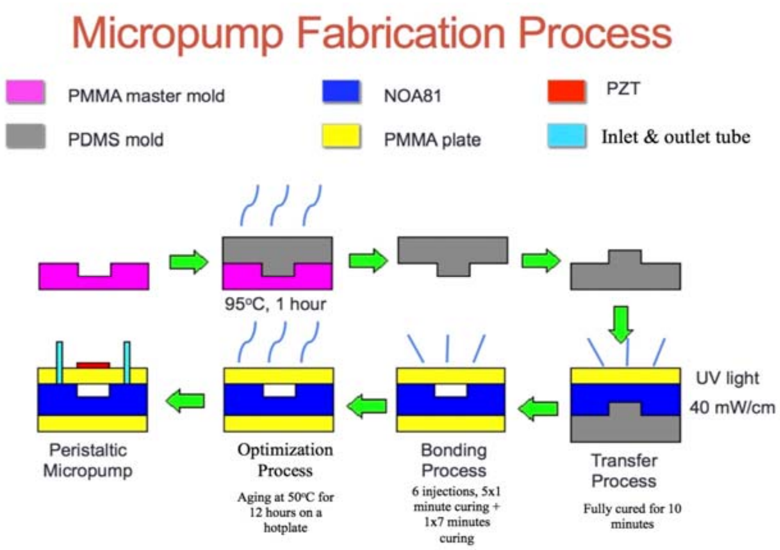

Fig.1 Schematic diagram of the peristaltic micropump fabrication process

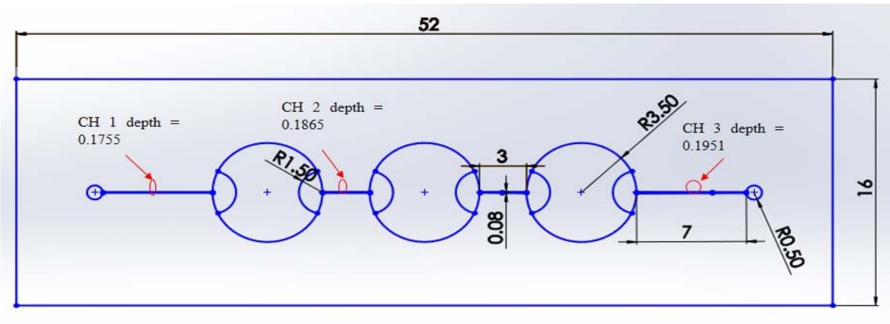

Fig.2 Peristaltic micropump geometries (in millimeters)

(4) Bonding Process

The UV structure mold fabricated by the previous step was then sandwiched between two PMMA plates and clamped together to align inlet, outlet and chambers areas. Next, a slight amount of NOA81 liquid was injected into each side of the clamped PMMA plates using a syringe, up to six times injections. From the 1^{st} - 5^{th} injection, the NOA81 liquid was partially cured after each injection for 1 minute in order to prevent it from blocking the microchannels. After the 6^{th} injection, the NOA81 was fully cured for 7 minutes. After the exposure, the bond was optimized by aging at 50^{o}C for 12 hours, as a bonding optimization process.

(5) Final Micropump System

Three 6 mm square PZT plates were attached to glass substrates using silver epoxy to create PZT actuators. Actuators of PZT plates with known thickness of 191 μm were attached to UV adhesive based chambers by silver epoxy for electric contact.

2. Experimental Setups

(1) NOA81 Transfer Characteristics

The NOA81 will turn into its solid state by UV light curing for a certain period time, which is defined as fully cured state. If we cure the NOA81 before it reaches the fully cured state, the adhesive will only become sticky, which is defined as partially cured state. The post cured state is when the NOA81 was cured again after it reached the fully cured state.

A confocal microscopy (KEYENCE, VK-X100/X200) was used to measure the geometry accuracy between partially cured, fully cured and post cured NOA81 mold. These molds were compared with PMMA master mold. The maximum error tolerance is set to be 10%. In this experiment, the fully cured period of the NOA81 was also determined based on the geometry accuracy. The target areas of this investigation consist of four spots, three channels' centers and one edge of the middle chamber (Fig. 4).

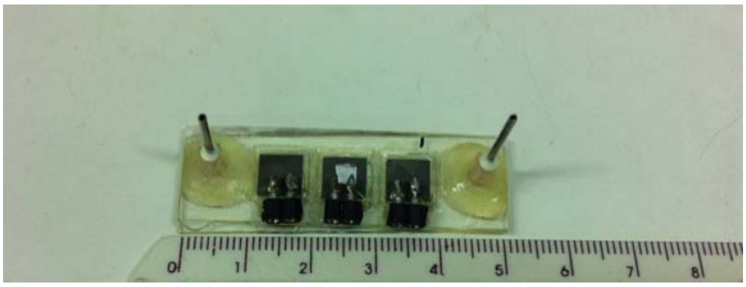

Fig.3 Completed UV adhesive based peristaltic micropump

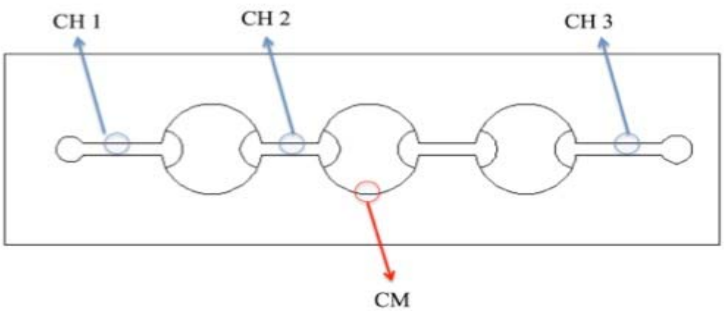

Fig. 4 The four spots for investigation under a confocal microscope

There were two conditions set in this experiments, such as: *Fully cured period*, the curing times were set to find the optimal results, which are 1 minute, 5 minutes, 10 minutes, 12 minutes, 15 minutes, 17 minutes, 20 minutes, 25 minutes, 30 minutes, 40 minutes, 50 minutes and 60 minutes; *Consistency of the NOA81 mold geometry*, the depths of five fully cured molds by the same curing process were measured for four times. The geometrical errors from these experiments were calculated using:

$$Error = \left(\frac{NOA81_{depth} - PMMA_{depth}}{PMMA_{depth}} \right) \times 100\% \cdot \qquad (1)$$

(2) Bonding Characteristics

The importance of a successful bonded wafer without flaws has to be considered. In this paper, bonding strength is the parameter to characterized wafer bonds.

Maszara *et al* [10] proposed a simple way to measure the bonding strength called razor blade method. A blade with known thickness is inserted between two wafers and the length of the resulting crack is measured. A formula was developed to correlate the crack length with bonding strength, in terms of surface energy by using equation below.

$$\gamma = \frac{3Et_w^3 t_b^2}{32L^4} \cdot \qquad (2)$$

where E is the Young's Modulus, t_w represents the thickness of the wafer and t_b is the blade's thickness and L is the crack's length.

The curing times were varied after the 6^{th} injection during the bonding process. Five different curing times for testing comparison were set to be: 1 minute, 3 minutes, 5 minutes, 7 minutes and 10 minutes. Based on [11], the optimum adhesion can be achieved by aging at 50^{o}C for 12 hours on a hotplate. In this experiment, the bonding strength from unoptimized an optimized adhesion were measured. For *first condition (un-optimized)*, razor blades were directly inserted after curing. For *second condition (optimized)*, after curing, samples were heated on a hotplate at 50^{o}C for 12 hours, then razor blades were inserted into the bonded samples.

(3) Peristaltic Micropump Performance

The peristaltic micropump was actuated by function generator and power amplifier. The membrane displacement was measured using a fiber optic measurement system (MTI Instrument, MTI 2000 Fotonic Sensor). The fotonic sensor probe was positioned above middle PZT actuator and aligned above the center of the PZT actuator. The flow rate was estimated by a microbalance to measure the change in weight of the fluid over a period of time. The pumping fluid was DI water and the experimental processes commenced at 100 V_{pp} , peak to peak voltage, and frequencies ranging from 25 to 400 Hz.

The maximum backpressure of the micropump was measured by gradually raising the height of the output relative to the micropump's altitude. And the height of the output, until the flow rate reduced to zero, is termed maximum backpressure. In this experiment, the micropump was driven by a constant voltage of 100 V_{pp} at 37.5 Hz. The pumping fluid was DI water.

III.Results and Discussions

1. NOA81 Transfer Characteristics

Based on the experimental observation (Table 1) under the confocal microscope, the 1 minute and 5 minutes samples both have errors exceed the maximum tolerance (10%), while 10 minutes sample only does not

Table 1. Comparison of depths errors between PMMA master mold and NOA81 molds for different UV curing time

Curing time	CH 1 (%)	CH 2 (%)	CH 3 (%)	CM (%)	Average (%)	Std. deviation (%)
1 minute	0.522	11.127	-6.226	8.529	3.488	7.892
5 minutes	6.126	17.602	8.281	15.943	11.988	5.635
10 minutes	4.418	-1.757	-4.157	-4.646	-1.535	4.165
12 minutes	-41.73	-46.468	-46.122	16.949	-29.343	30.936
15 minutes	-8.969	0.493	-27.584	-5.782	-10.461	12.074
17 minutes	-0.532	-12.575	-8.577	-4.991	-6.669	5.131
20 minutes	-8.658	-35.289	3.317	3.077	-9.388	18.149
25 minutes	-2.071	-6.121	23.968	-16.157	-0.095	17.099
30 minutes	-3.269	0.007	-0.231	0.881	-0.653	1.809
40 minutes	0.611	-12.397	-6.331	6.106	-3.002	8.069
50 minutes	-2.338	-8.268	-2.582	-4.791	-4.495	2.747
60 minutes	0.556	0.099	-8.265	-4.874	-3.121	4.219

Table2. Consistency testing results of the average values of five samples from depths measurements of fully cured NOA81 structure molds (10 minutes UV curing)

Area	1st measurement (μm)	2nd measurement (μm)	3rd measurement (μm)	4th measurement (μm)	Std. dev. (μm)
CH 1	183.466	176.386	177.703	176.679	3.32
CH 2	183.173	186.703	184.276	186.903	1.835
CH 3	186.945	196.756	194.744	196.478	4.611
CM	13.851	14.612	14.932	14.95	0.514

exceed 10 % error tolerance. Longer curing time samples (12 minutes, 15 minutes, up to 40 minutes) have errors exceed 10% tolerance. 1 minute sample was with 11.13% error on CH 2, 5 minutes sample was with 17.6% error on CH 2 and 15.94% on CM. It shows that, after 1 minute and 5 minutes curing, the NOA81 does not completely turn into its solid state yet. As a result, during the peeling process, a slight amount of pressure can effect the structure's geometry. Thus, this study demonstrates that the NOA81 will reach the fully cured state in 10 minutes UV light curing.

Post curing has an effect on the geometry of the NOA81 structure molds. Longer curing time will not guarantee good replication results. Table 1 exhibits most of the post cured NOA81 molds have bad geometry replication. Based on this reason, during the fabrication process, the NOA81 structure mold was cured for 10 minutes in order to get a good replication result with a short amount of time.

For the consistence tests, the 5 fully cured samples were prepared and measured for four times. The average values from the four times measurements were shown in Table 2. Table 2 also exhibits standard deviation of 5 fully cured samples from four times measurement on each target area. For channel area, the biggest std. deviation is 4.611 μm on CH 3 spot. Compared with the channel's depth, this value is relatively small. Meanwhile, std. deviation for chamber area is 0.514 μm, which is very small. It shows the consistency of the NOA81 to replicate a microstructure, thus NOA81 is an applicable material to replicate microstructure.

Table3. Razor blade test results

No.	Curing time (minute)	Crack length (mm)	Surface energy (J/m^2)
1.	1*	27	0.19 ± 0.01
2.	3	20	0.64 ± 0.06
3.	5	16	1.55 ± 0.18
4.	7	15	2.01 ± 0.25
5.	10	13	3.56 ± 0.5
6.	H 1**	19	0.78 ± 0.07
7.	H 3	15	2.01 ± 0.25
8.	H 5	12	4.9 ± 0.74
9.	H 7	10	10.16 ± 1.8
10.	H 10	10	10.16 ± 1.8

* First condition samples; 1 stands for sample with 1 minute curing time; 3 stands for sample with 3 minutes curing time and so on

** Second condition samples; H 1 means that the sample was UV cured for 1 minute, then the sample was heated on a hotplate at 50^{o}C for 12 hours; H 3 means that the sample was UV cured for 3 minutes, then the sample was heated on a hotplate at 50^{o}C for 12 hours and so on

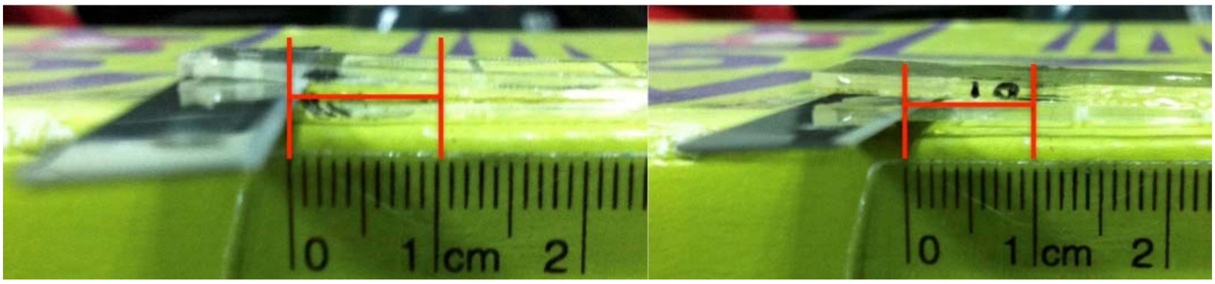

Fig. 5 Crack length for H 7 sample (left); crack length for H 10 sample (right)

2. Bonding Characteristics

The parameters of E, t_b and t_w for calculating the surface energy are 3.1 GPa, 0.45 mm and 1.2 mm, respectively.

The standard deviation for crack length measurement was 0.5 mm. Among all of the samples, the highest surface energy can be achieved is 10.16 J/m^2 from the optimized sample. Table 1 indicates optimized samples surface energy values are four times bigger than unoptimized samples. The surface energy from H 7 and H 10 sample are the same, because they have the same crack length (Fig. 5). Thus, in the bonding process, the micropump's main body was fully cured for 7 minute and heated for 12 hours at 50^{o}C on a hotplate (Fig. 1) in order to achieve the highest surface energy. Typical values of adhesive surface energy for non-toughened adhesive are of the order of 10-100 J/m^2, with 1 mm adhesive layer thickness [12]. Because the NOA81 surface energy is in between the typical values, there is no flaw in the bonding process.

3. Peristaltic Micropump Performance

The maximum membrane displacement and flow rate are 0.824 μm and 21.87 μ/min, respectively, achieved at 37.5 Hz. The highest backpressure of the UV adhesive based micropump is 4.42 Pa. Previous work from Cheng [9] (PMMA based peristaltic micropump with the same design), the maximum flow rate and backpressure are 133.6 μl/min and 11.8 Pa, respectively. Cheng's micropump has deeper channels than the micropump of this paper. Theoretically, shallower depth produces bigger fluidic resistance, as a result the flow rate is smaller. Next, the NOA81 has lower Young's Modulus (1.38 GPa) [8] than PMMA's (3.1 GPa). During the actuation process, the NOA81 structure deforms under a force from PZT actuators; thus, the backpressure was smaller.

IV. Conclusions

The first workable UV adhesive based peristaltic micropump was fabricated. The NOA81 was served both as a part of micorpump main body and a bonding material.

Under a confocal microscope, the geometry accuracy of NOA81 structure molds was investigated. From this experiment, the NOA81 reached the fully cured state in 10 minutes time under UV light curing. The consistency of the fully cured NOA81 mold was tested. Five fully cured NOA81 molds were prepared and measured for four times. Standard deviation of each target area from all the measurements was calculated. The standard deviation on channels and chamber areas are very small compared to channels and chamber depths. As a result, NOA81 is an applicable material to replicate micropump's channel and chamber. In this work, the highest NOA81's bonding strength is 10.16 J/m^2, achieved at 7 minutes of UV light curing and heated at 50^oC for 12 hours on a hotplate.

The maximum flow rate and backpressure are 21.87 μl/min and 4.42 Pa, respectively. Shallower channel produces bigger fluidic resistance, thus the micropump flow rate is small. NOA81 has low Young's Modulus, during the actuation process; the NOA81 structure undergoes a deformation, making the micorpump produces small backpressure.

References

[1] P. Woias. (2005). Micropumps-past, progress and future prospects, *Sensors and Actuators B, 105,* 28-38.

[2] N. T. Nguyen, X. Y. Huang and T. K. Chuan. (2002). MEMS-Micropumps: a Review, *J. Fluid Eng., 124*(2), 384-392.

[3] E. Sollier, C. Murray, P. Maoddi, and D. Di Carlo. (2011). Rapid Prototyping Polymers for Microfluidic Devices and High Pressure Injections, *Lab Chip*, *11*, 3752-3765.

[4] D. Bartolo, G. Degre, P. Nghe and V. Studer. (2008). Microfluidic Stickers, *Lab on a Chip*, *8*, 274-279.

[5] P. Wagli, A. Homsy, and N. F. de Rooij. (2010). *NOA81 for Fabrication of Microfluidic Devices With Adjustable Surface Properties and High Chemical Resistance Against IR-Transparent Organic Solvents*, Eurosensors XXIV Conference, Austria.

[6] E. P. Dupont, R. Luisier and M. A. M. Gijs. (2010). NOA63 as a UV-curable Material for Fabrication of Microfluidic Channels With Native Hydrophilicity, *Microelectronic Engineering*, *87*, 1253-1255.

[7] V. R. S. S. Mokkapati, O. Bethge, R. Hainberger and H. Brueckl. (2012/05/29~2012/06/01). Microfluidic Chips Fabrication from UV Curable Adhesives for Heterogeneous Integration, 1965-1969. Electronic Components and Technology Conference (ECTC), 2012 IEEE 62nd, San Diego, California.

[8] Norland Optical Adhesive Information, http://www/norlandprod.com/UVdefault.html. (retrieved date: 2014/07/14)

[9] P. Y. Cheng. (2014). *Unsaturated Polyesters as Stamps for Hot Embossing of Micropumps* (Master Thesis), Southern Taiwan University of Science and Technology, Tainan, Taiwan.

[10] W. P. Maszara *et al*. (1988). Bonding of Silicon Wafers for Silicon-on-Insulator, *J. Appl. Phys*, *99*, *4943*.

[11] Norland Optical Adhesive Information, http://www.norlandproducts.com/adhesives/noa%2081.html. (retrieved date: 2014/07/14)

[12] A. J. Kinloch. (1987). *Adhesion and Adhesives Science and Technology,* New York: Chapman and Hall.

[13] Y. C. Hsu *et al*. (2007). Applying Taguchi Methods for Solvent-Assistant PMMA bonding technique for static and dynamic m-TAS devices, *Biomedical Microdevices, 9*(4), 513-522